ORIGINAL RESEARCH

Comprehensive Analysis of scRNA-Seq and Bulk RNA-Seq Reveals Transcriptional Signatures of Macrophages in Intrahepatic Cholestasis of Pregnancy

Mi Tang[1,2,*], Liling Xiong[3,*], Jianghui Cai[2,4,*], Xuejia Gong[2], Li Fan [iD][1], Xiaoyu Zhou[1], Shasha Xing[1], Xiao Yang [iD][3]

[1]Chengdu Women's and Children's Central Hospital, School of Medicine, University of Electronic Science and Technology of China, Chengdu, 611731, People's Republic of China; [2]School of medicine, University of Electronic Science and Technology of China, Chengdu, People's Republic of China; [3]Obstetrics Department, Chengdu Women's and Children's Central Hospital, School of Medicine, University of Electronic Science and Technology of China, Chengdu, 611731, People's Republic of China; [4]Department of Pharmacy, Chengdu Women's and Children's Central Hospital, School of Medicine, University of Electronic Science and Technology of China, Chengdu, 611731, People's Republic of China

*These authors contributed equally to this work

Correspondence: Shasha Xing; Xiao Yang, Chengdu Women's and Children's Central Hospital, School of Medicine, University of Electronic Science and Technology of China, Chengdu, 611731, People's Republic of China, Email xingshasha1230@126.com; wcchgcptg@163.com

Purpose: Intrahepatic cholestasis of pregnancy (ICP) is a disorder that characterized by maternal pruritus, abnormal liver function, and an elevation in total bile acid concentrations during pregnancy. Immune factors have been recognized as playing a vital role in the mechanism of ICP. However, the underlying mechanisms regulating dysfunctional immune cells and immune genes remain to be fully elucidated.

Patients and Methods: Single-cell RNA sequencing and bulk RNA sequencing data of the placenta were downloaded from the SRA database. The AUCell package, Monocle package and SCENIC package were utilized to explored immune cell activity, cell trajectory and transcription factor, respectively. GO, KEGG, and GSEA were employed to explore potential biological mechanisms. Cell-cell communications were further investigated using the CellChat package. RT-PCR, and Western blot were used to verify the gene expression in placenta.

Results: In placenta cells, macrophages were found to be significantly increased in ICP. Additionally, macrophages exhibited the highest immune gene score and were divided into four subclusters (MF1-4). Our analysis revealed significant elevations in MF2, associated with LPS response and antigen presentation, and MF4, associated with TNF and cytokine production. MF3 displayed an anti-inflammatory phenotype. MF1, closely related to ribosomes and proteins, exhibited a sharp decrease. Although ICP maintained an anti-inflammatory state, macrophage trajectories showed a gradual progression toward inflammation. Subsequently, we confirmed that cytokine- and chemokine-related signaling pathways were emphasized in macrophages. Within the CXCL signaling pathway, the increased expression of CXCL1 in macrophages can interact with CXCR2 in neutrophils, potentially inducing macrophage infiltration, stimulating neutrophil chemotaxis, and leading to an inflammatory response and cellular damage.

Conclusion: In conclusion, we firstly revealed the transcriptional signatures of macrophages in ICP and discovered a tendency toward an inflammatory state. This study also provides new evidence that the CXCL1-CXCR2 axis may play an important role in the pathogenesis of ICP.

Keywords: intrahepatic cholestasis of pregnancy, scRNA-Seq, bulk RNA-Seq, immune gene, macrophage

Introduction

Intrahepatic cholestasis of pregnancy (ICP) is a disorder characterized by maternal pruritus, abnormal liver function, and an elevation in total bile acid (TBA) concentrations during the second and third trimesters of pregnancy. This disease leads to adverse pregnancy outcomes such as meconium-stained amniotic fluid, premature delivery, and stillbirth. While ICP poses little risk for pregnant women and typically recovers after delivery, it increases susceptibility to hepatobiliary

cancer, immune diseases, and cardiovascular diseases.[1] The etiology of ICP remains poorly elucidated but likely involves a combination of genetic, hormonal, immunological, and environmental factors.

Immunological modifications have been recognized as primary to cholestasis, given that ICP is an inflammatory disorder.[2] Previous studies have indicated that increased TBA levels can shift the immune system from a normally TH2-mediated response to a TH1-mediated one,[3,4] which has been associated with more adverse pregnancy outcomes. TH1 and TH17-associated cytokines such as TNF-α, IFN-γ,[4] IL6,[5] IL8,[6] and IL17[7] have been found to increase, while TH2-associated cytokines such as IL4[3] and IL10 decrease. Furthermore, NK and NKT cells were found to increase in the decidua parietalis of ICP patients, while CD3+ T cells were decreased.[8] CD83+ dendritic cells (DCs) increased in the placenta of ICP patients, while decidual CD1a + DCs were significantly decreased.[9] Additionally, the presence of nuclear and smooth-muscle antibodies and an increase in anticardiolipin antibodies were also discovered in ICP.[10]

However, these findings were not sufficient to systematically and comprehensively analyze the changes of immune cells during the disease process, particularly macrophages. Macrophages play a pivotal role in the progression of pregnancy. They are abundant in placental tissue and have the ability to phagocytose and clear the surrounding apoptotic cells. Macrophages contribute significantly to pregnancy by supporting connective tissue remodeling and spiral arteries formation, promoting trophoblast cell invasion, and protecting the fetus from microbial invasion.[11]

In this study, we performed bioinformatics analysis combining scRNA-seq and bulk RNA-seq data to explore the expression characteristics and possible regulatory mechanisms of immunity, particularly macrophages in ICP.

Methods
scRNA Sequencing Data Processing

The raw data (SRP429602) were aligned to the human reference genome (GRCh38) and processed using CellRanger (version 7.1.0) to generate a feature-barcode gene expression matrix. A total of 18,972 cells were included for analysis. R (version 4.2.2) combined with the Seurat R package (version 4.3.0) was utilized for downstream analysis, with a minimum of 3 cells required per group. Cells with nFeature_RNA ≤200, nFeature_RNA ≥10000, or mitochondrial genes ≥25% were filtered out. Following data normalization, 2000 highly variable genes (HVGs) were identified, and Principal component analysis (PCA) was conducted and visualized using JackStraw and ElbowPlot. Subsequently, 15 principal components (PCs) were selected for Uniform Manifold Approximation and Projection (UMAP) analysis, with a resolution set to 0.3. Differentially expressed genes (DEGs) in each cluster were identified using the FindAllMarkers function, with an average natural logarithm (fold change) threshold of 0.25. Cell types were determined based on the top 10 DEGs and manually verified according to a previous study.[12–14] In the subcluster analysis of macrophages, 15 PCs were selected for UMAP analysis, with a resolution set to 0.2.

Bulk Sequencing Data Processing

The raw data from SRP378990 were downloaded from the EMBL-EBI database. FASTQ files underwent quality control to ensure a per base sequence quality greater than 30 and were aligned to the human reference genome GRCh38 using HISAT2 (https://daehwankimlab.github.io/hisat2/) for comparison. Subsequently, SAM files were converted to BAM files and sorted by chromosome position. The gene annotation file GRCh38 was obtained from GENCODE (https://www.gencodegenes.org/), and raw counts were obtained using FEATURECOUNTS. Quality control and DEG analysis were conducted using the R package DESeq2 (version 1.38.3). DEGs with padj < 0.05 and |log2foldchange| > 1 were considered significantly dysregulated genes. Volcano plots were generated using the ggplot2 package (version 3.4.3).

Immune Genes Score

AUCell (Version 1.20.2)[15] was utilized to identify cells with immune gene activity in the single-cell RNA data. Initially, a ranking was built based on the single-cell expression matrix, and a gene set comprising 571 immune genes was generated by screening DEGs of each cell (padj < 0.05) using the ImmPort database (https://www.immport.org/shared/home). Subsequently, the area under the curve (AUC) was calculated using the top 10% of genes in the ranking, with cells expressing more immune genes within the gene set receiving higher AUC values.

Assignment thresholds were set to identify gene set active cells. Finally, the AUC score for each cell was mapped onto UMAP for visualization using the ggplot2 package (version 3.4.3).

Cell Trajectory Analysis

Monocle 2 (version 2.26.0)[16] was employed to sequence single cells in "pseudotime" and position them on an inferred trajectory. Reversed Graph Embedding was utilized to reduce the dimensionality of data and calculate the pseudo-time of cells.

Transcription Factor (TF) Identification

Transcription factor regulation was predicted using SCENIC (version 1.3.1).[15] Co-expression network calculations were conducted using the GENIE3 package, transcription factor potential binding motifs were analyzed using the RcisTarget package, and regulator activity scores of each cell were calculated using the AUCell package.

Functional Enrichment Analysis

The intersection of DEGs from SRP378990 (padj < 0.05 and |log2foldchange| > 1) and DEGs of the macrophage cluster (padj < 0.05) from SRP429602 was independently imported into the Xiantao online tools (https://www.xiantao.love/) for Gene Ontology (GO) and Kyoto Encyclopedia of Genes and Genomes (KEGG) analysis. The top 3 pathways were selected based on the adjusted p-value (padj) ranking. Additionally, gene set enrichment analysis (GSEA) was conducted using the clusterProfiler package (version 4.6.2).[17] Gene set variation analysis (GSVA) was performed with the GSVA package (version 1.46.0).[18]

Cell-Cell Interaction Analysis

CellChat was utilized to calculate and analyze intercellular communication between the ICP and normal groups.[19] The cells were categorized into three clusters: immune cells, trophoblast cells, and other cells, for analysis. Furthermore, to elucidate the strength of specific pathways among macrophages, CCL, CXCL, IL1, IL10, IL16, IL6, and TNF signaling pathways were selected for further visualization. Additionally, ligand-receptor interactions between macrophages and other cells were analyzed in depth.

RNA Extraction and RT-PCR

The collection of placenta samples from participants was approved by The Ethics Committee of the Chengdu Women's and Children's Central Hospital (Number: 2022(49)-2), following the guidelines outlined in the Declaration of Helsinki. Informed consents were obtained from the participants. RNA was extracted from placentas using TRIzol reagent (Invitrogen, Carlsbad, CA, USA) and then reverse transcribed using the PrimeScript™ RT reagent Kit with gDNA Eraser (Takara, Japan). RT-PCR was performed using TB Green™ Premix Ex Taq™ II (Takara, Japan). The primers contained CXCL1, CXCR2 and GAPDH (Supplementary Table S1). Relative mRNA levels were calculated using the 2-ΔΔCT method.

Western Blot Analysis

Protein was extracted from placental tissue using radioimmunoprecipitation assay (RIPA) and phenylmethanesulfonyl fluoride (PMSF). The protein concentration was quantified using the Pierce BCA Protein Assay Kit (Beyotime, Shanghai, China). Proteins were separated by 12.5% SDS-PAGE (Yamei, Shanghai, China) and transferred onto PVDF membranes. After blocking with nonfat dry milk (Yili), the membranes were immunoblotted with primary antibodies overnight at 4∘C. The antibodies used were anti-CXCL1 (Abcam, Cambridge, UK, ab206411), anti-CXCR2 (Proteintech, Wuhan, China, 20634-1-P), anti-GAPDH (Proteintech, Wuhan, China, 60004-1-Ig).

Statistical Analysis

ImageJ (National Institutes of Health, Rockville, MD) was used for processing Western blot data. All analyses, including Western blot, PCR, and clinical data, were completed using Prism (GraphPad; San Diego, CA). Statistically significant differences were assessed by *t*-test.

Results

Placental Cell Composition

To investigate specific alterations in ICP at the placental single-cell level, we analyzed raw scRNA-seq data from 2 placental tissues at the maternal-fetal interface (from one ICP patient and one healthy pregnant woman) in the SRA database, resulting in 7882 cells from ICP and 11,090 cells from the healthy group. Quality control (Figure S1A) was performed, and then cells were filtered to obtain 7601 cells from ICP and 10,834 cells from the healthy group, respectively. The nCount_RNA, representing the number of unique molecular identifiers (UMI), was positively correlated with nFeature_RNA, representing the number of genes, with a correlation coefficient of 0.87 (Figure S1B). The top 10 high HVGs (Figure S1C) were identified, and the linear dimension reduction algorithm PCA was applied to obtain the heatmap (Figure S1D), JackStrawPlot (Figure S1E), and ElbowPlot (Figure S1F). As a result, 15 PCs were selected for uniform manifold approximation and projection (UMAP) analysis, generating 19 clusters (Figure 1A). Moreover, all differentially expressed genes (DEGs) in each cluster were identified (Supplementary Table S2).

According to previous studies,[11] these clusters were assigned to the corresponding cell lineages by marker genes (Figure 1B and C). The final 15 identified cell types (Figure 1D) included: Macrophage (markers: CD68, CD163), Fibroblast (markers: DLK1, IGFBP3), NK cell (markers: NCAM1, KLRB1), T cell (markers: CD3D, CD69), Neutrophil (markers: S100A8, CSF3R), DC (markers: CD80), Monocyte (markers: CD14), syncytiotrophoblast (SCT) (markers: GATA3), vascular endothelial cells (VEC, markers: CDH5, PECAM1), villous cytotrophoblast (VCT) (markers: EGFR, GATA3), decidualized stromal cells (DSC, markers: DKK1, IGFBP1), extravillous trophoblast (EVT) (markers: HLA-G), smooth muscle cells (SMC, markers: MYH11, NDUFA4L2), erythrocyte (markers: HBA1), and B cell (markers: CD19). Although ALAS2, HBA1, HBB, and HBG1 were differentially expressed in red blood cells, CCL2, CD14, IL1B, and CD69 were also enriched in erythrocyte. Therefore, fetal nucleated red blood cells may be included in this cluster.

Significant differences in placental cells between groups were observed in terms of composition and abundance (Figure 1E).

Immune Gene Activity of Placental Cells

To investigate the expression characteristics of immune genes in ICP placental cells, we first identified DEGs in each placental cell (padj < 0.05) and then intersected these genes with immune genes from the ImmPort database. Subsequently, a total of 271 intersecting immune genes were obtained (Supplementary Table S3). Higher AUC values indicate a yellow color, reflecting increased genes expression in the cells, predominantly concentrated in macrophages (Figure1F and 1G).

Subcluster of Macrophages

Based on the expression of specific surface markers from previous studies, macrophages can be roughly categorized into pro-inflammatory M1 macrophages and anti-inflammatory M2 macrophages. In our analysis, the M1-type marker CD80 was poorly expressed in ICP, while the M2-type markers CD163, CD209, and the soluble mediator IL10 were strongly expressed (Figure S2A). These findings align with previous reports[20,21] indicating that M1 macrophages gradually polarize into M2 macrophages as pregnancy progresses, with the latter becoming the dominant type.

In this study, MF1, MF2, MF3, and MF4 macrophages were obtained by subcluster analysis of macrophages (Figure 1H). The MF1 subcluster was particularly prominent in the normal group, whereas the MF2 subcluster was more apparent in the ICP group (Figure 1I and J).

MF1, MF2, and MF4 predominantly expressed markers of pro-inflammatory M1 macrophages, such as CD86, IL6R, IL1B, and IL1A (Figure 2A). Further KEGG and GO analysis revealed that MF1 was closely associated with ribosomes and proteins formation (Figure 2B and Supplementary Table S4), and GSVA analysis exhibited that MF1 was also related to antibody-dependent cellular cytotoxicity and MHC class II receptor activity (Figure 2F). KEGG and GO analysis showed that MF2 had a response to lipopolysaccharide (LPS) and was closely related to the MHC class II protein complex (Figure 2C and Supplementary Table S5), MF4 was closely associated with positive regulation of cytokine production, leukocyte proliferation, and TNF signaling pathway (Figure 2E and Supplementary Table S6). Notably, IL6
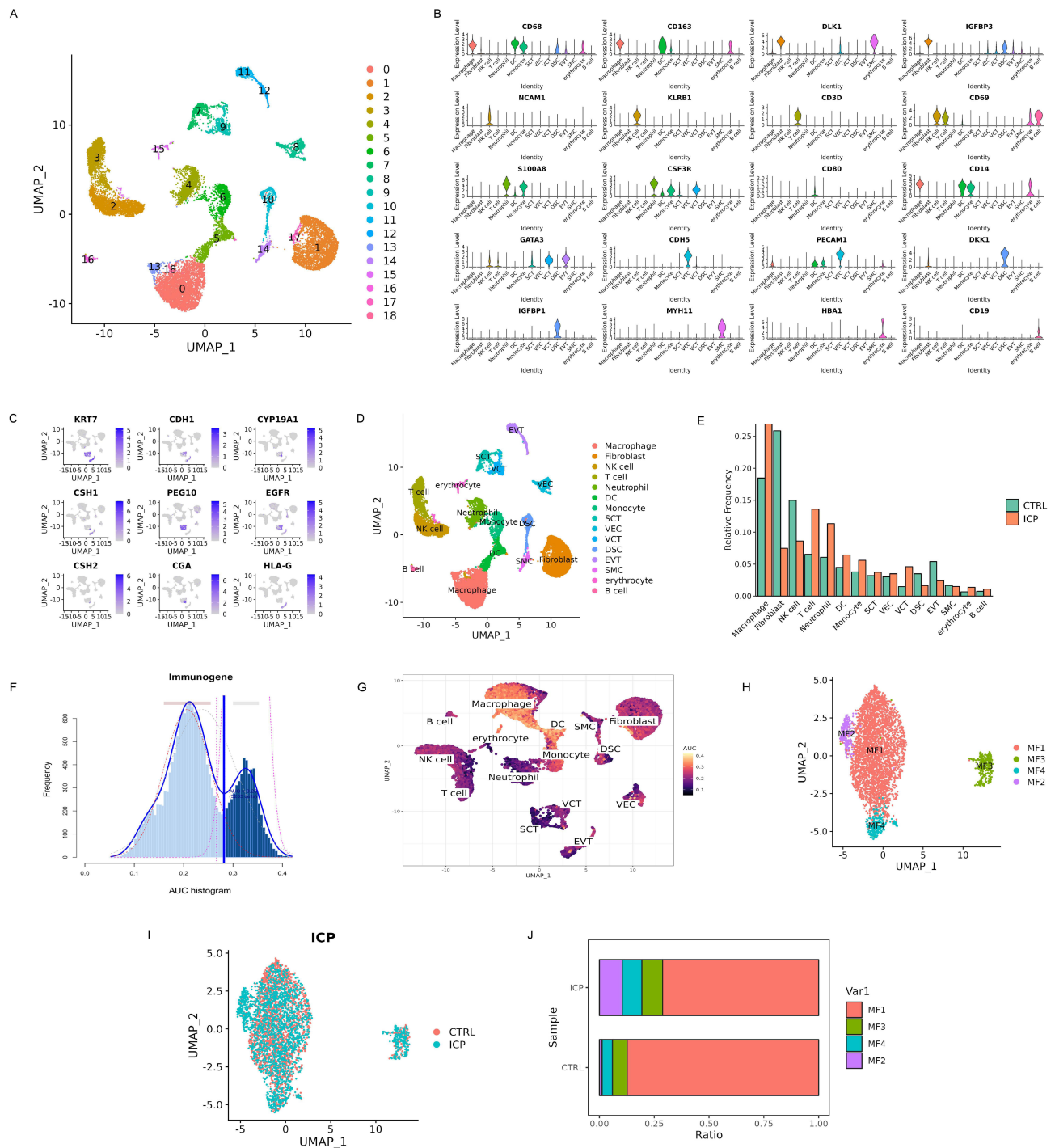
Figure 1 Placenta cells in ICP. (**A**) UMAP analysis of scRNA-seq data. (**B**) Violin plot of marker genes in placenta cells. (**C**) FeaturePlot of marker genes in trophoblast cells. VCT (markers: KRT7, PEG10, EGFR, CYP19A1, CDH1), SVT (markers: KRT7, CSH2, CGA, CYP19A1, CSH1), EVT (markers: KRT7, HLA-G, CDH1, CSH1). (**D**) Clusters annotation and cell types identification via UMAP. (**E**) Cell distribution in control and ICP groups. (**F**) Score of 271 screened immunogene. The threshold was chosen as 0.28. (**G**) UMAP of Immunogene score in all clusters. As regulon is conceptually defined as a set of target genes regulated by a transcription factor, AUC values represent the activity of Regulons in cells. Macrophage and DC cells express more genes and exhibit higher AUC values. (**H**) Subcluster of macrophages via UMAP. (**I**) Distribution of Macrophages in each group. (**J**) Subcluster of macrophages in each group.

was highly expressed in MF4 (Figure 2A). GSVA analysis exhibited that MF2 and MF4 were related with myeloid dendritic cell chemotaxis (Figure 2G) and negative regulation of interleukin-6 mediated signaling pathway (Figure 2I), respectively. On the other hand, MF3 exhibited characteristics indicative of anti-inflammatory M2 macrophages and mainly expressed M2-type markers CD209 and CD163 (Figure 2D and Supplementary Table S7). MF3 was closely
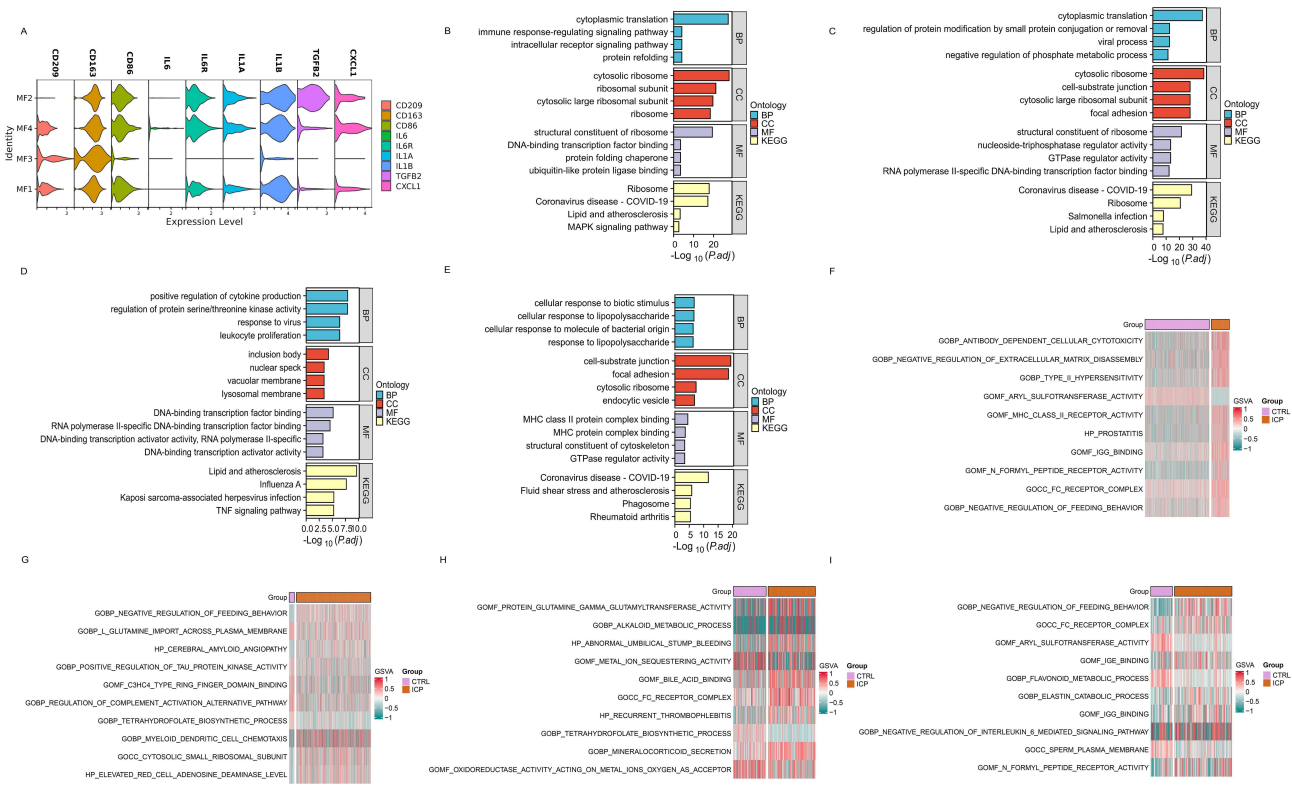
Figure 2 Enrichment analysis of macrophages in ICP. (**A**) Marker gene expression of each subcluster in macrophage. (**B–E**) The top 4 GO analysis and KEGG analysis of DEGs in MF1, MF2, MF3 and MF4 cluster. GO analysis includes three parts: Molecular Function (MF), Biological Process (BP) and CellComponent (CC). (**F–I**) GSVA analysis of MF1, MF2, MF3 and MF4 cluster.
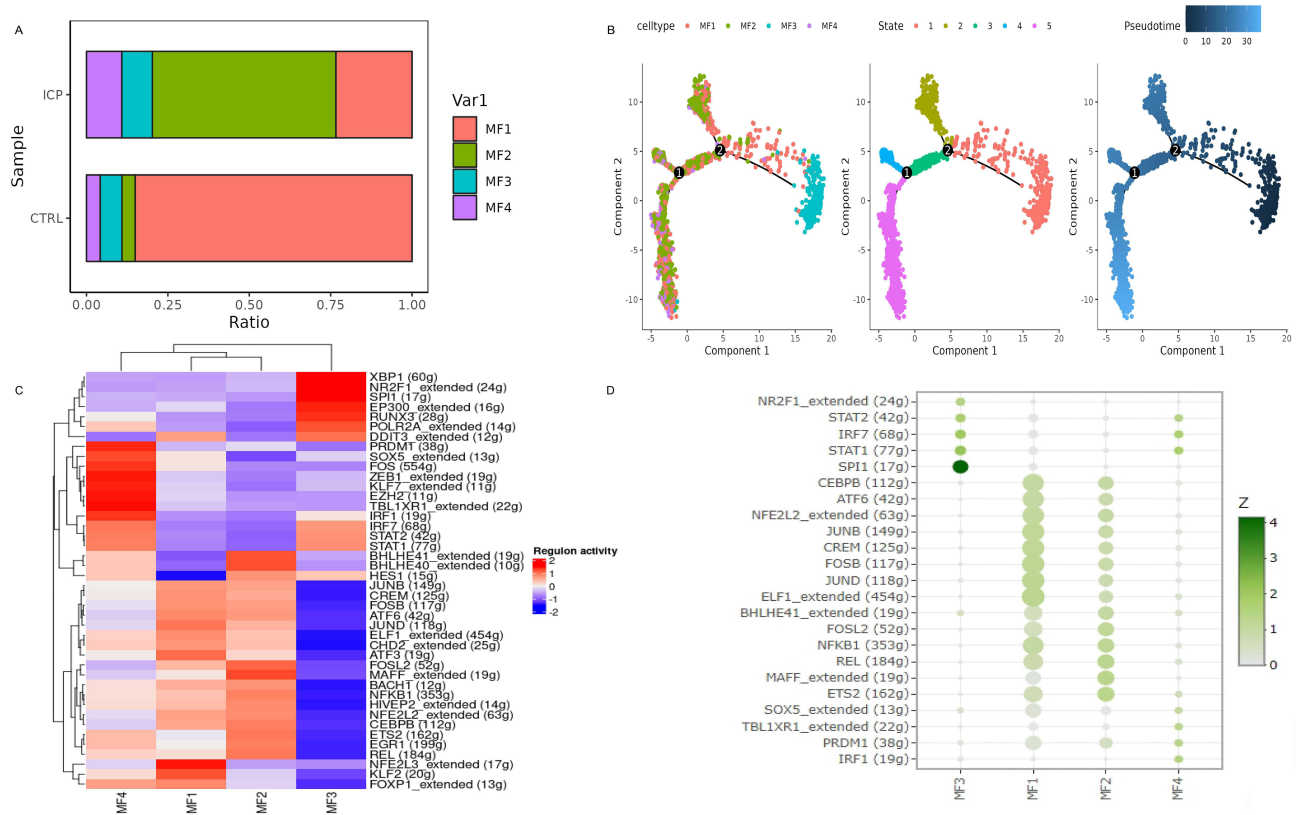
related to bile acid binding (Figure 2H). Interestingly, MF3 showed a weak relationship with growth factors, such as marker gene CXCL1, TGFB2, IL6, IL1B, and IL1A were rarely expressed in this subcluster (Figure 2A).

Trajectory Analysis and Transcription Factor Regulatory Network of Macrophages

Although previous findings indicated that macrophages in ICP remained in an immunosuppressive state dominated by M2 macrophages, our analysis revealed significant elevations in MF2, associated with LPS response and antigen presentation, and MF4, associated with TNF and cytokine production. Conversely, MF1, closely related to ribosomes and proteins, exhibited a sharp decrease (Figure 1J). Furthermore, cell trajectory analysis indicated that anti-inflammatory MF3 primarily existed at the beginning, while MF1 and MF2 existed in the end stage of temporal development, ultimately leading to a predominance of macrophages in an inflammatory state (Figure 3B).

SCENIC analysis was performed to investigate the underlying molecular mechanisms of placental cells in ICP, especially macrophages. Regulon relative activity was visualized to explore the relationship between cells and regulon (Figure S2B and Supplementary Table S8), and Regulon Specificity Score (RSS)[22] was calculated to evaluate cell specificity. This analysis revealed that each subcluster of macrophages was characterized by a unique transcription factor network (Figure 3C, 3D and Supplementary Table S9).

MF1 and MF2 exhibited a high degree of overlap and similarity in regulon. The MF2 subcluster-specific BHLHE40 and BHLHE41 activities significantly increased, believed to be involved in the control of cell differentiation. In the MF1 subcluster, NFE2L3 and KLF2 activity significantly increased, while HES1 decreased. HES1 acts as a transcriptional repressor of genes that require a bHLH protein for their transcription. Additionally, regulon relative activity and RSS of NR2F1 and SPI1 relative activity were specifically increased in MF3, while SOX5, TBL1XR1, PRDM1, and IRF1 were significantly increased in MF4.

Figure 3 Trajectory analysis and transcription factor regulatory network of macrophages. (**A**) Cell distribution in each cluster. (**B**) Cell trajectory analysis of macrophages. (**C**) Heatmap of the inferred transcription-factor gene-regulatory networks of macrophages. (**D**) Regulon Specificity Score (RSS) is calculated to evaluate macrophage specificity. The dot size represents the RSS, higher RSS indicates stronger association between transcription factors and Regulon, besides, z-score can compare the specificity of the same regulon between different cell types.

Cell-Cell Communication

Cell-cell communication analysis was conducted to explore placenta cells, especially interactions between macrophages and other cells in ICP. We observed an increase in the number and weight of cell interactions in ICP patients (Figure S2C), including interactions involving macrophages (Figure S2D and S2E). Furthermore, when the 15 cell populations were divided into three groups, including the immune cell group, trophoblast cell group, and other cell group, the interaction between the immune cell group and the other two groups was significantly enhanced in ICP (Figure S2F).

To further explore macrophage function, we analyzed Bulk RNA-seq data from twelve tissues (including seven ICP and five normal placenta tissues)[23] to obtain DEGs (padj < 0.05 and |log2foldchange| > 1) (Figure 4A). We then combined these DEGs with genes expressed in macrophages, resulting in 47 selected genes by intersection (Supplementary Table S10). GO and KEGG analysis of these intersected genes were performed (Supplementary Table S11 and Figure 4B), focusing on chemokine pathways. GSEA analysis further confirmed the enrichment of the cytokine-cytokine receptor interaction pathway in ICP (Figure 4C). As a result, further analysis revolved around cytokine and chemokine signaling pathways in cell-cell communication (Figure S2G), including IL10, IL6, TNF, CCL, and CXCL signaling pathways.

In ICP patients, IL10RA in the IL10 pathway was found to be decreased both in macrophages (Figure 5A and B) and in bulk RNAseq data (Figure 5C). Additionally, IL6 signaling and TNF signaling pathways were significantly enhanced (Figure 5D and E). IL6R in IL6 signaling, and TNF, TNFRSF1B in TNF signaling were both increased in macrophages, while IL6ST in IL6 signaling and TNFRSF1A in TNF signaling were attenuated (Figure 5F and G), consistent with the expression trend in ICP (Figure 5H and I). Besides, in the cell communication within macrophage subclusters, the IL6 signaling pathway was significantly increased in ICP (Figure 5J), and the role of MF1 and MF2 in the TNF signaling pathway was enhanced (Figure 5K).
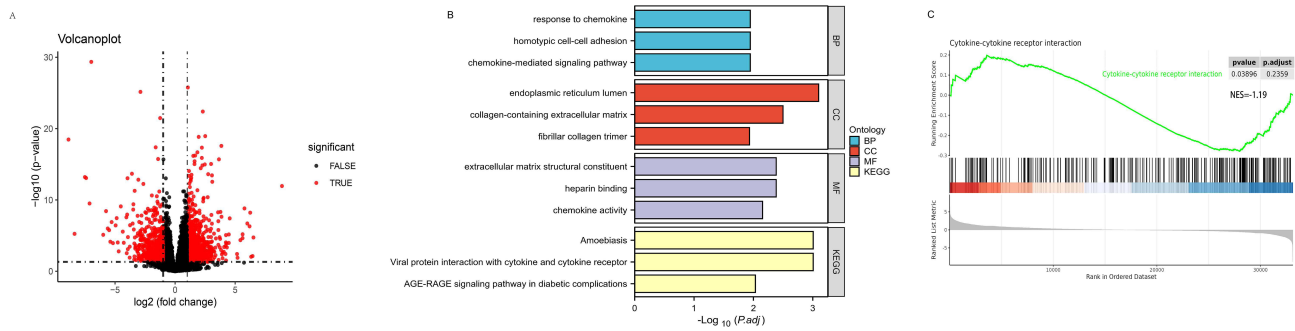
Figure 4 Placenta genes from SRP378990 dataset. (**A**) Volcano plot of DEGs in Bulk RNA-seq data. Up-regulated genes and down-regulated genes were colored in red. (**B**) The top 3 GO and KEGG of analysis of DEGs in SRP378990 dataset. (**C**) GSEA analysis of Cytokine-cytokine receptor interaction in SRP378990 dataset.
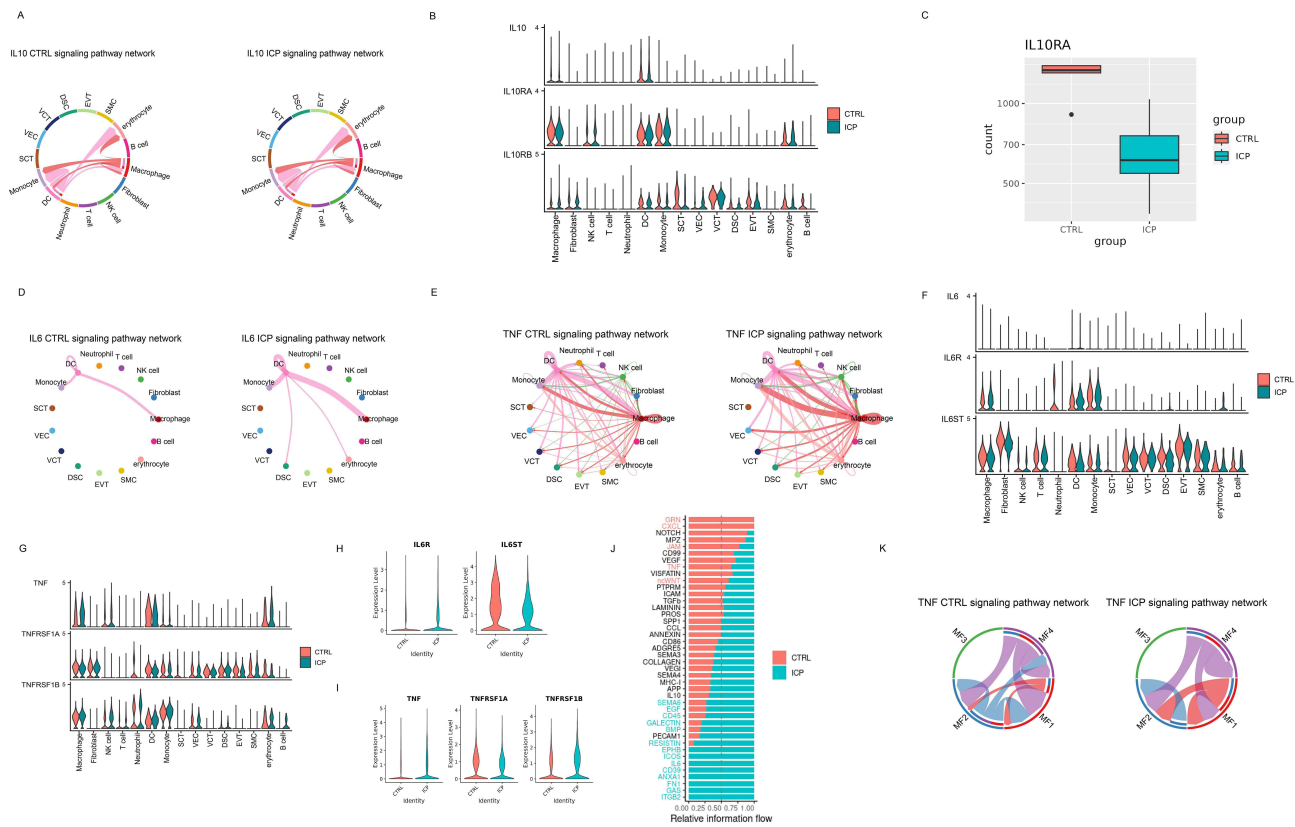

Figure 5 Cell-cell communication changes in cytokine related pathways. In cell-cell communication, the pathways revolved around cytokine includes IL10, IL6, TNF signaling pathways. (**A**) Chord diagram of IL10 signaling pathway network in placenta cell-cell communication. (**B**) Gene expression of IL10 signaling pathway in placenta cell-cell communication. (**C**) Expression of gene IL10RA in Bulk RNA-seq data. (**D** and **E**) Circle plot of IL6 and TNF signaling pathway network in placenta cell-cell communication. (**F** and **G**) Gene expression of IL6 and TNF signaling pathway in placenta cell-cell communication. (**H** and **I**) Expression of gene IL6, IL6ST, TNF, TNFRSF1A and TNFRSF1B in scRNA-seq data. (**J**) Enrichment degree of cellular pathways in macrophage subgroups. (**K**) Chord diagram of IL10 signaling pathway network in cell-cell communication of macrophage subgroups.

Furthermore, CCL signaling was enhanced in macrophages (Figure 6A). Although the expression of CCL3, CCL8, CCL2, and CCL4 in signaling was decreased in macrophages (Figure 6B) and bulk RNA-seq data (Figure S3A–S3D), CCL5 and CCL20 were increased (Figure S3E–S3F). Conversely, CXCL signaling was attenuated in macrophages (Figure 6C). CXCL2, CXCL8, and CXCL16 expression was attenuated in macrophages (Figure 6D) and bulk RNA-seq data (Figure S3G–S3I), while CXCL1 expression was enhanced (Figure 6D). Notably, CXCL1-CXCR2, the ligand receptor of macrophages and neutrophils, was elevated in ICP (Figure 6E). Furthermore, we observed the expression changes of CXCL1 in macrophages
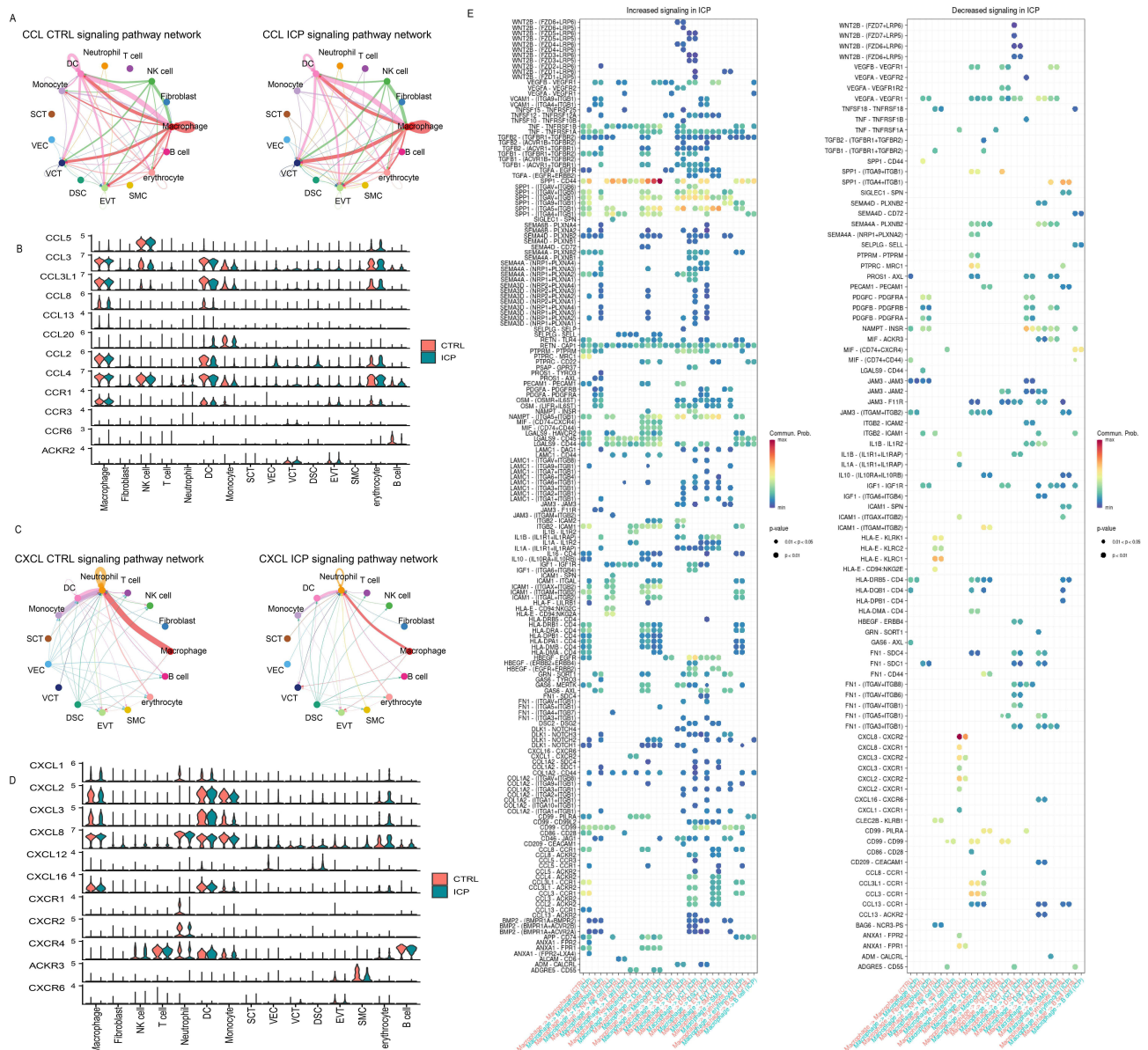
Figure 6 Cell-cell communication changes in chemokine related pathways. In cell-cell communication, the pathways revolved around chemokine includes CCL and CXCL signaling pathways. (**A**) Circle plot of CCL signaling pathway network in cell-cell communication. (**B**) Gene expression of CCL signaling pathway in cell-cell communication. (**C**) Circle plot of CXCL signaling pathway network in cell-cell communication. (**D**) Gene expression of CXCL signaling pathway in cell-cell communication. In ICP, the expression of CXCL1 is enhanced in macrophage. (**E**) Bubble plot of ligand receptor pairs of macrophages interacting with other cells. CXCL1-CXCR2, the ligand receptor of macrophages and neutrophils, is elevated in ICP.

during ICP, and depicted CXCL1 in cell trajectory of macrophages (Figure 7A and 7B). The upregulation of CXCL1 and CXCR2 was confirmed by bulk RNA-seq data, RT-QPCR, and Western blot (Figure 7C–E and Supplementary Table S12).

Discussion

Although immune factors have been identified as pivotal in the pathogenesis of ICP, limited knowledge exists regarding the alterations of immune cells within the placenta. Our study unveiled significant changes in placental cell composition in ICP. Notably, trophoblast cells exhibited an increase in VCT and SCT, whereas EVT was decreased, potentially impairing vascular remodeling during pregnancy. Among immune cells, NK cells decreased, while macrophages, neutrophils, and T cells increased. This aligns with prior findings of increased CD19+ B cells in the placenta of ICP
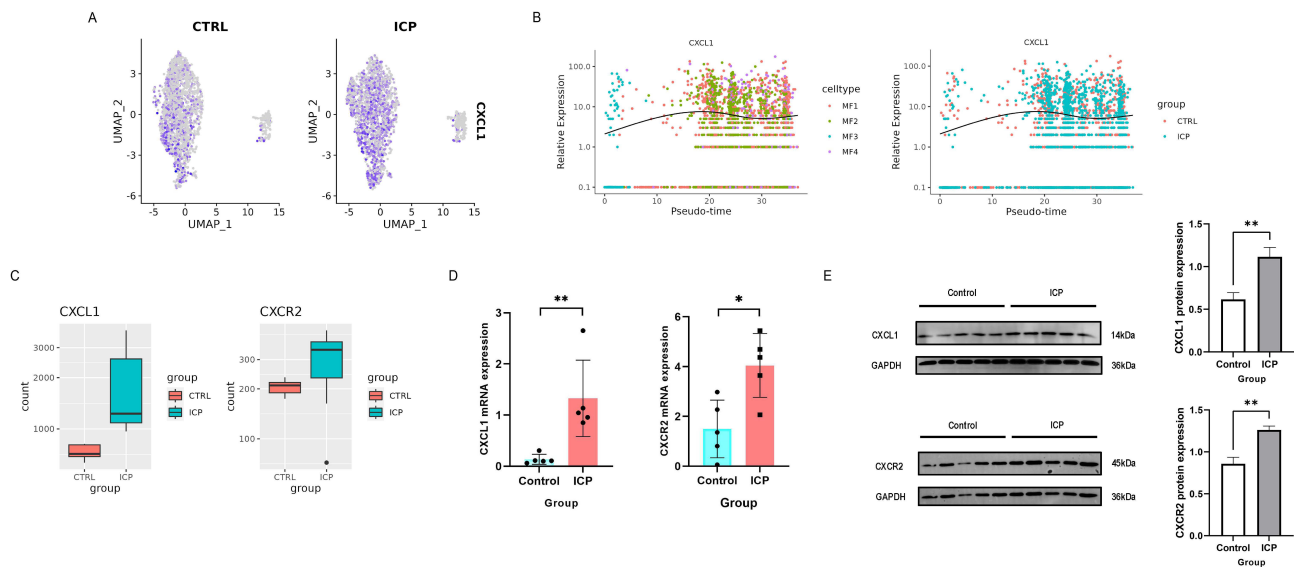
Figure 7 Expression of gene CXCL1 and CXCR2 in ICP. (**A**) FeaturePlot of gene CXCL1 in macrophages. (**B**) The cell trajectory of CXCL1 in macrophages. (**C**) Expression of gene CXCL1 and CXCR2 in Bulk RNA-seq data.(**D**) The QRT-PCR data shows the gene expression levels of CXCL1 and CXCR2 in control and ICP placentas (n = 5 in the control group and ICP group). * P<0.05,** P<0.01. (**E**) Western blot data shows the gene expression levels of CXCL1 and CXCR2 in control and ICP placentas (n = 5 in the control group and ICP group).

patients,[24] corroborated in our study. Enhanced interactions between immune cells and trophoblast cells, particularly by macrophages with heightened immune gene activity, were observed in ICP.

Further exploration into the function of macrophages delineated four subclusters. The decrease in MF1, associated with protein formation, contrasted with the notable increase in MF2, linked to LPS response and antigen presentation. Macrophages play a crucial role in initiating the immune response by presenting antigens to other immune cells. External stimuli such as LPS are known to promote M1 polarization. Additionally, transcription factors BHLHE40 and BHLHE41, which were involved in cell differentiation, significantly increased in the MF2 subcluster. The MF3 cluster exhibited characteristics of M2-type macrophages, with elevated production of CD163 and CD209, known for their immunosuppressive properties and involvement in biological activities such as scavenging debris and modulating inflammatory responses. Moreover, MF3 rarely expressed genes related to growth factors. The MF4 cluster was involved in cytokine production, leukocyte proliferation, and the TNF signaling pathway, displaying characteristics of M1-type macrophages, such as high expression of CD86 and IL6.[25–27] Despite the placental immunosuppressed state in ICP, the increase in MF2 and MF4, especially the rapid rise in MF2, illustrated the inflammatory nature of the disease process.

Furthermore, MF4 was closely associated with the TNF signaling pathway and significantly increased the expression of IL6. Previous studies have demonstrated that TNF-α can induce the production of IL-6 during states of inflammation. Elevated levels of IL6 have been associated with various aspects of ICP, including recurrent miscarriage and preterm birth.[28,29]

Moreover, upon integrating bulk RNA-seq data from the ICP placenta, emphasis was placed on cytokine and chemokine-related signaling pathways in macrophages. Cell-cell communication analysis highlighted the significance of the chemokine signaling pathway in the pathogenesis of ICP. CXCL1-CXCR2, the ligand receptor of macrophages and neutrophils, increased in ICP. This elevation was further confirmed by bulk RNA-seq data and experiments involving RT-PCR and Western blot.

Furthermore, CXCL1 was found to increase significantly in MF2 macrophages in ICP. Lee et al demonstrated the role of CXCL1 in angiogenesis and trophoblast invasion by decidual macrophages.[30,31] CXC is a major subfamily of chemokines, which are secondary pro-inflammatory mediators regulated by primary pro-inflammatory mediators such as IL-1 and TNF.[32] The subsequent release of CXC chemokines was chemotactic for neutrophils.[33] Our findings were consistent with previous studies, indicating that the subsequent release of CXC chemokines can activate neutrophils in circulation.[34] Additionally, some prospective case-control studies have reported a significantly higher neutrophil/

lymphocyte ratio in women with ICP.[35,36] During obstructive cholestasis in bile duct-ligated mice, the extravasation of neutrophils and reactive oxygen formation were responsible for the inflammatory injury.[37]

In conclusion, increases of CXCL1 in macrophages may interact with CXCR2, potentially inducing macrophage infiltration and stimulating neutrophil chemotaxis, leading to an inflammatory response and cellular damage. This study provides new evidence that the CXCL1-CXCR2 axis may play a vital role in the pathogenesis of ICP.

Abbreviations

ICP, Intrahepatic cholestasis of pregnancy; TBA, total bile acid; scRNA-seq, Single-cell RNA sequencing; bulk RNA-seq, bulk RNA sequencing; GO, Gene Ontology; KEGG, Kyoto Encyclopedia of Genes and Genomes; GSEA, Gene Set Enrichment Analysis; HVGs, highly variable genes; PCA, principal component analysis; PCs, principal components; UMAP, Uniform Manifold Approximation and Projection; DEGs, differentially expressed genes; UMI, unique molecular identifiers; LPS, lipopolysaccharide; MHC-II, MHC class II protein complex.

Funding

Disclosure

The authors have no relevant financial or non-financial interests to disclose.

References

1. Wikström Shemer EA, Stephansson O, Thuresson M, Thorsell M, Ludvigsson JF, Marschall HU. Intrahepatic cholestasis of pregnancy and cancer, immune-mediated and cardiovascular diseases: a population-based cohort study. *J Hepatol*. 2015;63:456–461. doi:10.1016/j.jhep.2015.03.010
2. Xiao J, Li Z, Song Y, et al. Molecular pathogenesis of intrahepatic cholestasis of pregnancy. *Can J Gastroenterol Hepatol*. 2021; 2021:6679322.
3. Yi J, Ding Y. Expression of HLA-G protein in placental tissues and its influence on Th1/Th2 cytokines in peripheral blood in patients with intrahepatic cholestasis of pregnancy. *Zhong Nan Da Xue Xue Bao Yi Xue Ban*. 2010;35:241–246. doi:10.3969/j.issn.1672-7347.2010.03.009
4. Peng B, Liu S. Study of relationship between T helper cell type-1 and type-2 cytokines and intrahepatic cholestasis of pregnancy. *Zhonghua Fu Chan Ke Za Zhi*. 2002;37:516–518.
5. Zhang Y, Hu L, Cui Y, et al. Roles of PPARγ/NF-κB signaling pathway in the pathogenesis of intrahepatic cholestasis of pregnancy. *PLoS One*. 2014;9:e87343.
6. Çelik S, Guve H, Çalışkan C, Çelik S. The role of melatonin, IL-8 and IL-10 in intrahepatic cholestasis of pregnancy. *Z Geburtshilfe Neonatol*. 2021;225:238–243. doi:10.1055/a-1233-9084
7. Kirbas A, Biberoglu E, Ersoy AO, et al. The role of interleukin-17 in intrahepatic cholestasis of pregnancy. *J Matern Fetal Neonatal Med*. 2016;29:977–981. doi:10.3109/14767058.2015.1028354
8. Ling B, Yao F, Zhou Y, Chen Z, Shen G, Zhu Y. Cell-mediated immunity imbalance in patients with intrahepatic cholestasis of pregnancy. *Cell Mol Immunol*. 2007;4:71–75.
9. Kong X, Kong Y, Zhang F, Wang T, Zhu X. Expression and significance of dendritic cells and Th17/Treg in serum and placental tissues of patients with intrahepatic cholestasis of pregnancy. *J Matern Fetal Neonatal Med*. 2018;31:901–906. doi:10.1080/14767058.2017.1300652
10. Ylöstalo P, Kurki T, Pietarinen I, Järvinen T, Mäkitalo R. Mitochondrial, nuclear and smooth-muscle antibodies in intrahepatic cholestasis of pregnancy. *Ann Chir Gynaecol*. 1978;67:206–209.
11. Hazan AD, Smith SD, Jones RL, Whittle W, Lye SJ, Dunk CE. Vascular-leukocyte interactions: mechanisms of human decidual spiral artery remodeling in vitro. *Am J Pathol*. 2010;177:1017–1030. doi:10.2353/ajpath.2010.091105
12. Vento-Tormo R, Efremova M, Botting RA, et al. Single-cell reconstruction of the early maternal-fetal interface in humans. *Nature*. 2018;563:347–353. doi:10.1038/s41586-018-0698-6
13. Suryawanshi H, Morozov P, Straus A, et al. A single-cell survey of the human first-trimester placenta and decidua. *Sci Adv*. 2018;4:eaau4788. doi:10.1126/sciadv.aau4788
14. Liu Y, Fan X, Wang R, et al. Single-cell RNA-seq reveals the diversity of trophoblast subtypes and patterns of differentiation in the human placenta. *Cell Res*. 2018;28:819–832. doi:10.1038/s41422-018-0066-y
15. Aibar S, González-Blas CB, Moerman T, et al. SCENIC: single-cell regulatory network inference and clustering. *Nat Methods*. 2017;14:1083–1086. doi:10.1038/nmeth.4463
16. Qiu X, Mao Q, Tang Y, et al. Reversed graph embedding resolves complex single-cell trajectories. *Nat Methods*. 2017;14:979–982. doi:10.1038/nmeth.4402
17. Yu G, Wang LG, Han Y, He QY. clusterProfiler: an R package for comparing biological themes among gene clusters. *Omics*. 2012;16:284–287. doi:10.1089/omi.2011.0118

18. Hänzelmann S, Castelo R, Guinney J. GSVA: gene set variation analysis for microarray and RNA-seq data. *BMC Bioinf*. 2013;14:7. doi:10.1186/1471-2105-14-7

19. Jin S, Guerrero-Juarez CF, Zhang L, et al. Inference and analysis of cell-cell communication using cellChat. *Nat Commun*. 2021;12:1088. doi:10.1038/s41467-021-21246-9

20. Zhang YH, He M, Wang Y, Liao AH. Modulators of the balance between M1 and M2 macrophages during pregnancy. *Front Immunol*. 2017;8:120. doi:10.3389/fimmu.2017.00120

21. Gustafsson C, Mjösberg J, Matussek A, et al. Gene expression profiling of human decidual macrophages: evidence for immunosuppressive phenotype. *PLoS One*. 2008;3:e2078. doi:10.1371/journal.pone.0002078

22. Davie K, Janssens J, Koldere D, et al. A single-cell transcriptome atlas of the aging drosophila brain. *Cell*. 2018;174:982–998.e920. doi:10.1016/j.cell.2018.05.057

23. Wang Y, Tang Y, Yang X, et al. Immune dysfunction mediated by the ceRNA regulatory network in human placenta tissue of intrahepatic cholestasis pregnancy. *Front Immunol*. 2022;13:883971. doi:10.3389/fimmu.2022.883971

24. Du Q, Pan Y, Zhang Y, et al. Placental gene-expression profiles of intrahepatic cholestasis of pregnancy reveal involvement of multiple molecular pathways in blood vessel formation and inflammation. *BMC Med Genomics*. 2014;7:42. doi:10.1186/1755-8794-7-42

25. Mantovani A, Sica A, Sozzani S, Allavena P, Vecchi A, Locati M. The chemokine system in diverse forms of macrophage activation and polarization. *Trends Immunol*. 2004;25:677–686. doi:10.1016/j.it.2004.09.015

26. Tang MX, Hu XH, Liu ZZ, Kwak-Kim J, Liao AH. What are the roles of macrophages and monocytes in human pregnancy? *J Reprod Immunol*. 2015;112:73–80. doi:10.1016/j.jri.2015.08.001

27. Nagamatsu T, Schust DJ. The contribution of macrophages to normal and pathological pregnancies. *Am J Reprod Immunol*. 2010;63:460–471. doi:10.1111/j.1600-0897.2010.00813.x

28. Prins JR, Gomez-Lopez N, Robertson SA. Interleukin-6 in pregnancy and gestational disorders. *J Reprod Immunol*. 2012;95:1–14. doi:10.1016/j.jri.2012.05.004

29. Larson SP, Kovilam O, Agrawal DK. Immunological basis in the pathogenesis of intrahepatic cholestasis of pregnancy. *Expert Rev Clin Immunol*. 2016;12:39–48. doi:10.1586/1744666X.2016.1101344

30. Belperio JA, Keane MP, Arenberg DA, et al. CXC chemokines in angiogenesis. *J Leukocyte Biol*. 2000;68:1–8. doi:10.1189/jlb.68.1.1

31. Lee CL, Guo Y, So KH, et al. Soluble human leukocyte antigen G5 polarizes differentiation of macrophages toward a decidual macrophage-like phenotype. *Hum Reprod*. 2015;30:2263–2274. doi:10.1093/humrep/dev196

32. Ohira H, Abe K, Yokokawa J, et al. Adhesion molecules and CXC chemokines in endotoxin-induced liver injury. *Fukushima J Med Sci*. 2003;49:1–13. doi:10.5387/fms.49.1

33. Graves DT, Jiang Y. Chemokines, a family of chemotactic cytokines. *Crit Rev Oral Biol Med*. 1995;6:109–118. doi:10.1177/10454411950060020101

34. Bajt ML, Farhood A, Jaeschke H. Effects of CXC chemokines on neutrophil activation and sequestration in hepatic vasculature. *Am J Physiol Gastrointest Liver Physiol*. 2001;281:G1188–1195. doi:10.1152/ajpgi.2001.281.5.G1188

35. Kirbas A, Biberoglu E, Daglar K, et al. Neutrophil-to-lymphocyte ratio as a diagnostic marker of intrahepatic cholestasis of pregnancy. *Eur J Obstet Gynecol Reprod Biol*. 2014;180:12–15. doi:10.1016/j.ejogrb.2014.05.042

36. Oztas E, Erkenekli K, Ozler S, et al. Can routine laboratory parameters predict adverse pregnancy outcomes in intrahepatic cholestasis of pregnancy? *J Perinat Med*. 2015;43:667–674. doi:10.1515/jpm-2014-0207

37. Gujral JS, Farhood A, Bajt ML, Jaeschke H. Neutrophils aggravate acute liver injury during obstructive cholestasis in bile duct-ligated mice. *Hepatology*. 2003;38:355–363. doi:10.1053/jhep.2003.50341